

Final report

Study and advanced study of edge isolation with the waterjet guided laser

Dr. B. Richerzhagen

Synova S.A.

Chemin de la Dent D'Oche

1024 Ecublens

by Dipl.-Ing. Sybille Baumann

and Dr. Daniel Kray

1 Experimental proceeding

125 commercial solar cells were bought from a german cell manufacturer whereof 95 cells exhibited no edge isolation (EI). First, illuminated and dark IV-curves were measured to specify the input parameters.

15 cells were used afterwards to find the optimum parameters for the EI process with the waterjet-guided laser. 70 cells were then edge isolated with the Synova-System (LaserMicroJet™ (LMJ) with the Spectron IR-laser) and 10 cells with a UV-laser (355 nm) with flying optics. In the latter case one has to note that the process wasn't fully optimized yet.

The following process variants were realized:

1. Standard-industry-EI 1 (performed by the cell manufacturer), approx. 10 μm cutting depth
2. LMJ, IR-laser, 13 kHz, 40.4 W, 250 mm/sec, front side (FS)-EI, approx. 20 μm cutting depth
3. LMJ, IR-laser, 13 kHz, 40.4 W, 250 mm/s, back side (BS)-EI, approx. 20 μm cutting depth
4. LMJ, IR-laser, 13 kHz, 22.8 W, 250 mm/s, FS-EI, approx. 5 μm cutting depth
5. LMJ, IR-laser, 13 kHz, 22.8 W, 250 mm/s, BS-EI, approx. 5 μm cutting depth
6. LMJ, IR-laser, 20 kHz, 45.2 W, 250 mm/s, FS-EI, approx. 20 μm cutting depth
7. LMJ, IR-laser, 20 kHz, 45.2 W, 250 mm/s, BS-EI, approx. 20 μm cutting depth
8. LMJ, IR-laser, 20 kHz, 23.9 W, 250 mm/s, FS-EI, approx. 5 μm cutting depth
9. LMJ, IR-laser, 20 kHz, 23.9 W, 250 mm/s, BS-EI, approx. 5 μm cutting depth
10. LMJ, IR-laser, 13 kHz, 40.4 W, 100 mm/s, FS-EI, approx. 40 μm cutting depth
11. LMJ, IR-laser, 20 kHz, 45.2 W, 100 mm/s, FS-EI, approx. 45 μm cutting depth
12. ISE-EI with flying optics UV-laser, not fully optimized, approx. 8 μm cutting depth

After edge isolation illuminated IV-curves of the cells were measured and for respectively 4 cells of the parameter groups 2, 3, 4, 5, 6, 7 and 12 also dark IV-curves were measured.

Additional SunsVoc and thermography measurements (under V_{OC} and MPP conditions as well as dark thermography) were performed at a few cells of different parameter groups.

Thereafter all cells were breakage tested (4-line-bending apparatus) and both optical microscope and SEM pictures were made from the laser grooves.

2 Results

Below the results of the studies are presented. The results refer to a little number of solar cells. For statistical relevant statements however several hundreds of solar cells for each parameter group are necessary and should be tested in a following study.

2.1 Electrical parameters

Table 1 shows that the electrical parameters of the LMJ edge isolation are comparable with the commercial lasers, i.e. the electrical quality of the reference process (standard-industry EI) can be achieved with the LMJ. For the dark IV-curves lower values of the second ideality factor n_2 can be fitted continuously. This indicates a reduced damage in the p-n-junction and emitter respectively.

The fact that LMJ process has obtained these results is very positive, because the process parameters of LMJ where suboptimal in some areas due to experimental restrictions:

- An IR-laser was used with LMJ instead of an UV-laser. This increases the penetration depth of the laser light.
- The corners of the solar cells are not isolated; only straight lines with a constant scanning speed could be processed in the LCS300.
- The width of the laser groove is 2-3 times wider than for the commercial laser systems since a 100 μm nozzle has been used, which increases accordingly the recombination losses.

For this reason one can expect better results for LMJ by using a UV light source and a smaller nozzle. To demonstrate this, further experiments have to be performed. Next steps for the industrial validation which are suggested from our side are described in the conclusion at the end of the report.

A very positive result is the successful edge isolation on the back side of the solar cell. This kind of isolation is preferred to the front side edge isolation in principle, because the active cell area is reduced in the latter case. With LMJ, nearly the same efficiencies as on the front side can be achieved. However the fill factor is still not optimal. But this is compensated by the increase of the short-circuit current (J_{SC}), see table 1 variant 2, 3 and 6, 7. With regard to the emitter damage J_{O_2} can be optimized as one can see on the thermography maps.

Table 1 also depicts that a 20 μm deep laser groove is sufficient for good edge isolation while a 5 μm deep groove seems to be too shallow. The laser frequency plays no important role for the LMJ. Both frequencies (13 kHz and 20 kHz) show good results. With a fast scanning speed of 250 mm/sec just as good results are obtained as with a lower scanning speed of 100 mm/sec. Consequently a 156x156 mm^2 solar cell could be edge isolated in $4 * 156 \text{ mm} / 250 \text{ mm/s} = 2.5 \text{ sec}$. Still higher scanning speeds for the used lasers are possible,

because a groove depth of 10 μm (compared to the standard lasers) is enough. A transfer rate of 1-2 sec per wafer is for this reason realistic for the LMJ.

The fill factor (FF) and efficiency increases are summarized in the following table:

Table 1: Electrical parameters of the edge isolation

El-variant	FF	ΔFF [% _{rel}]	stand. dev. [%]	J_{sc} [mA/cm ²]	$\Delta\eta$ [% _{rel}]	number of cells
1 standard-industry-EI 1	0,755			31,8		30
2 LMJ, IR-laser, 13 kHz, 40.4 W, 250 mm/s, FS-EI	0,751	+20,0	1,6	31,5	+22,0	7
3 LMJ, IR-laser, 13 kHz, 40.4 W, 250 mm/s, BS -EI	0,747	+19,4	1,2	31,8	+23,3	7
4 LMJ, IR-laser, 13 kHz, 22.8 W, 250 mm/s, FS-EI	0,688	+10,1	1,5	31,6	+11,4	7
5 LMJ, IR-laser, 13 kHz, 22.8 W, 250 mm/s, BS -EI	0,678	+8,5	1,4	31,4	+9,8	7
6 LMJ, IR-laser, 20 kHz, 45.2 W, 250 mm/s, FS-EI	0,760	+22,1	1,4	31,5	+24,0	7
7 LMJ, IR-laser, 20 kHz, 45.2 W, 250 mm/ s, BS -EI	0,744	+18,5	1,1	32,5	+21,8	7
8 LMJ, IR-laser, 20 kHz, 23.9 W, 250 mm/s, FS-EI	0,672	+6,8	1,2	32,1	+7,2	7
9 LMJ, IR-laser, 20 kHz, 23.9 W, 250 mm/s, BS -EI	0,652	+3,7	0,8	32,0	+4,4	7
10 LMJ, IR-laser, 13 kHz, 40.4 W, 100 mm/s, FS-EI	0,751	+19,7	2,0	32,0	+22,1	7
11 LMJ, IR-laser, 20 kHz, 45.2 W, 100 mm/s, FS-EI	0,748	+19,2	1,3	32,2	+21,3	7
12 ISE-EI with UV-laser	0,750	+19,8	1,6	31,9	+22,3	10

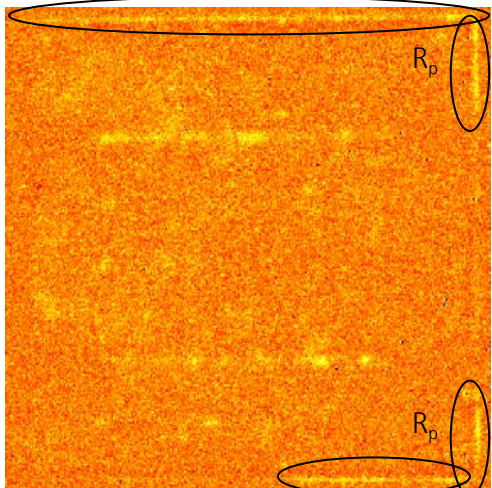
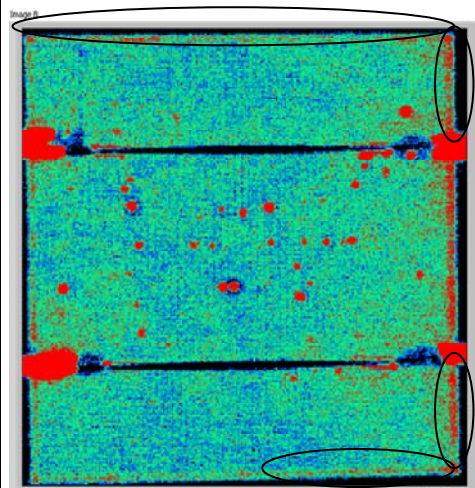
2.2 Thermography measurements

Shunts of solar cells under different operating conditions can be detected via thermography. In the case of edge isolation ohmic shunts can be distinguished from increased emitter recombination by comparison of thermography maps made in forward bias (V_{oc}) and reverse bias. An ohmic shunt exists if the current losses are visible in both kinds of maps because the direct connection of emitter and back side metallisation isn't separated completely (this becomes apparent by a reduced parallel resistance R_p). A diode shunt is responsible for the current losses if they appear only in one image. This can be explained e.g. by increased recombination in the p-n-junction (J_{02}).

The thermography images in table 2 depict that for the standard-industry-EI (variant 1) still ohmic shunts exists, whereas for LMJ (variant 2) they are removed¹.

For the edge isolations on the back side both kinds of shunts (R_p , J_{02}) are still present (variant 7). There is a demand of further optimization.

Table 2: Thermography measurements (left hand side V_{oc} , right hand side reverse bias)

Voc	Reverse bias
	
Sample I_2 EI_variant 1 (standard-industry process front side)	Sample I_2 EI_variant 1 (standard-industry process front side)

¹ One have to note that the edge isolated areas on the left and right hand side between the busbars can't be seen in the V_{oc} images because of technical measurement reasons.

<p>sample I_39 El_variant 2 (LMJ front side)</p>	<p>sample I_39 El_variant 2 (LMJ front side)</p>
<p>sample I_17 El_variant 7 (LMJ back side)</p>	<p>sample I_17 El_variant 7 (LMJ back side)</p>
<p>sample I_86 El_variant 12 (ISE UV)</p>	<p>sample I_86 El_variant 12 (ISE UV)</p>

2.3 SunsVoc measurements

A series resistance free IV-curve can be measured with SunsVoc which enables to find out the potential of the solar cell if the series resistance would be zero. With this one can appreciate the limitation of the cell by other parameters (R_p , J_{02}) which are directly influenced by the edge isolation.

The losses by series resistance are for all cells approximately equal as shown in table 3 for variant 1, 2, 7 and 12. This denotes that series resistances of the analyzed cells don't spread in a wide range and that they reduce the maximum achievable fill factors of approx. 5%_{rel.}

The stronger limitation of the fill factor to approx. 0.80 in variant 7 is caused by the not optimized p-n-separation on the back side edge isolation (LMJ). The limitation however is compensated by the increase in J_{sc} so that the efficiencies are comparable with the front side efficiencies of the LMJ edge isolated cells. With further optimization a process could eventually be achieved which exceed the front side process.

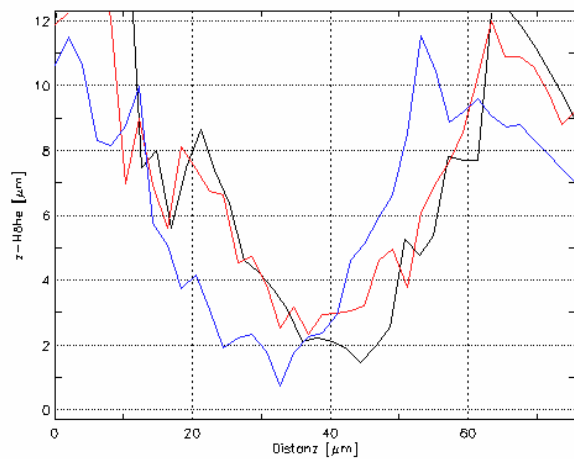
Table 3: Suns-Voc measurements FF_{pseudo}

El-variant		FF_{pseudo}	$\Delta FF = \frac{FF_{pseudo} - FF}{FF}$ [% _{rel}]
1	standard-industry-EI 1	0,820	4,9
2	LMJ, IR-laser, 13 kHz, 40.4 W, 250 mm/s, FS-EI	0,817	5,5
		0,816	4,7
7	LMJ, IR-laser, 20 kHz, 45.2 W, 250 mm/ s, BS -EI	0,804	5,2
		0,795	4,9
12	ISE-EI with UV-laser	0,813	5,3

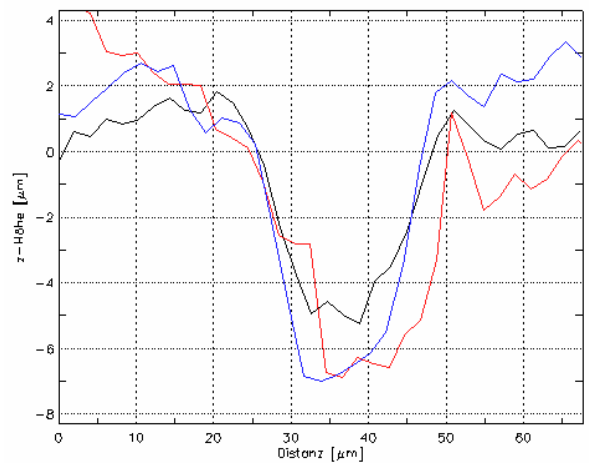
2.4 Comparison of the groove form (profile images)

Following images depict the groove profiles of different edge isolation variants, obtained with a FRT-MicroProf surface profiler. The different z-scales have to be considered.

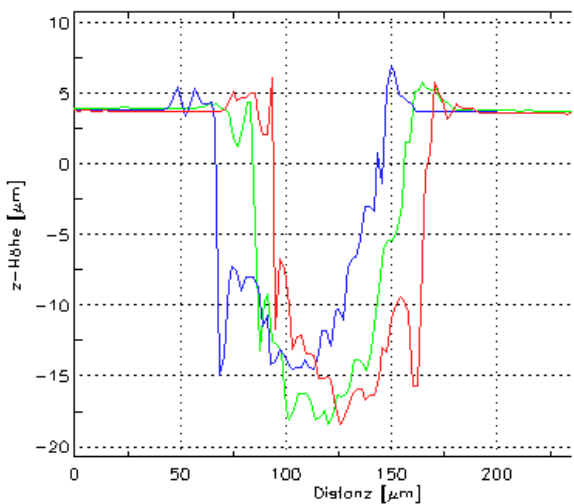
variant 1.:



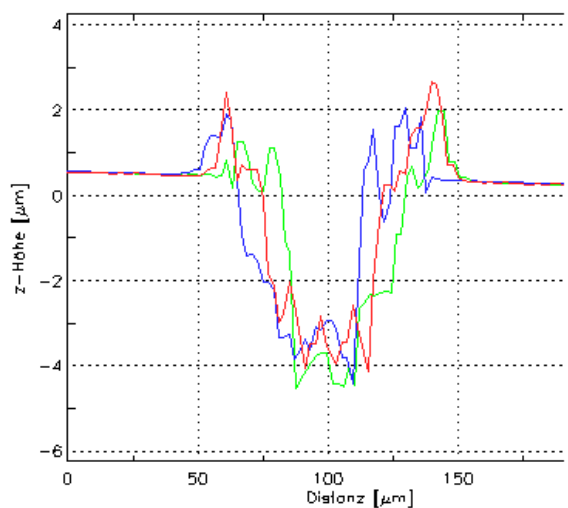
variant 12.:



variant 2.:

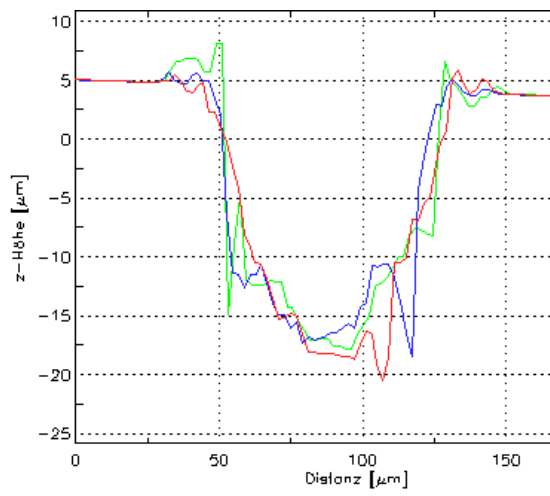


variant 4.:

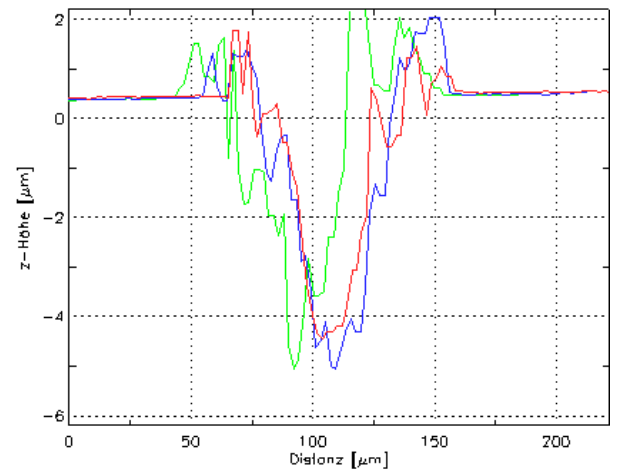




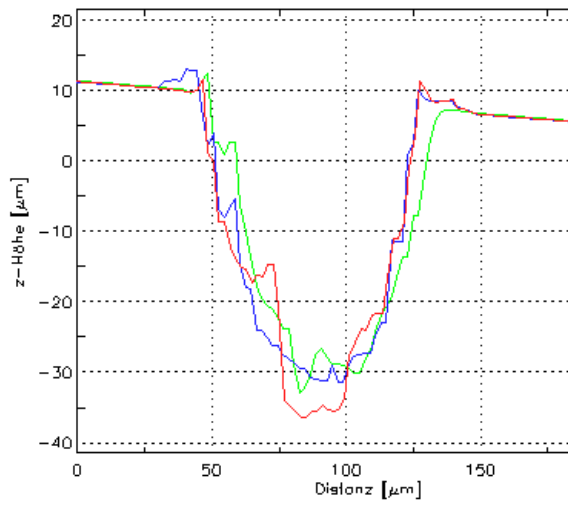
variant 6.:



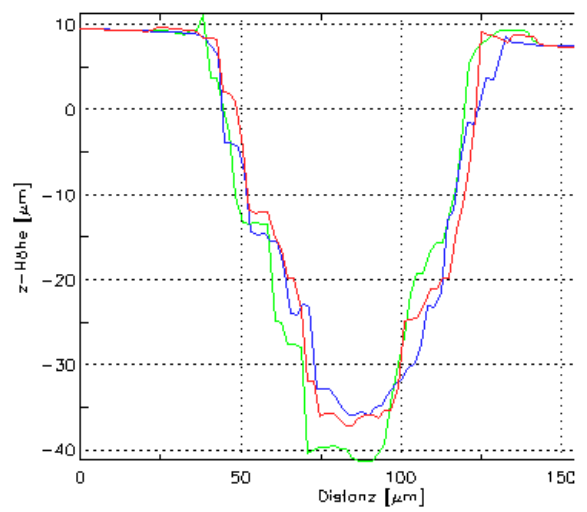
variant 8.:



variant 10.:

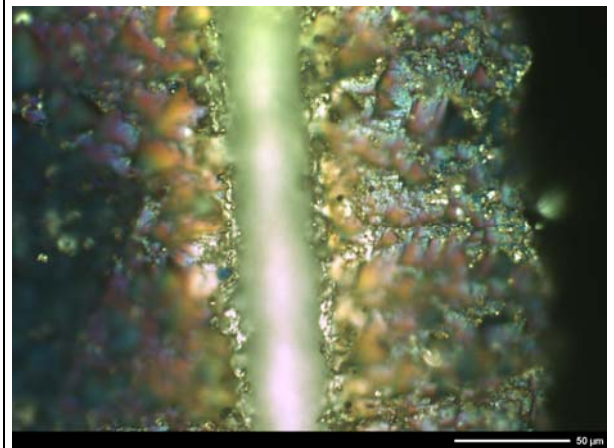
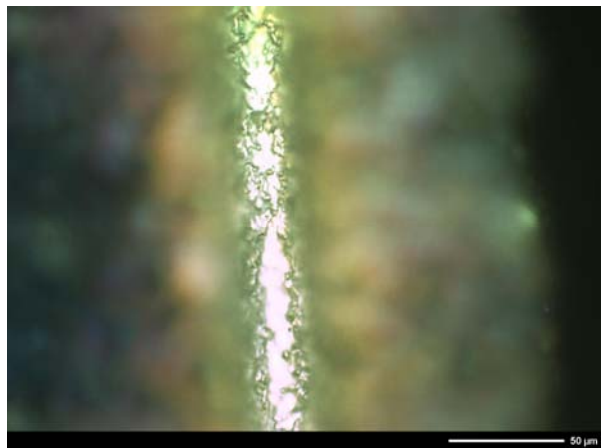
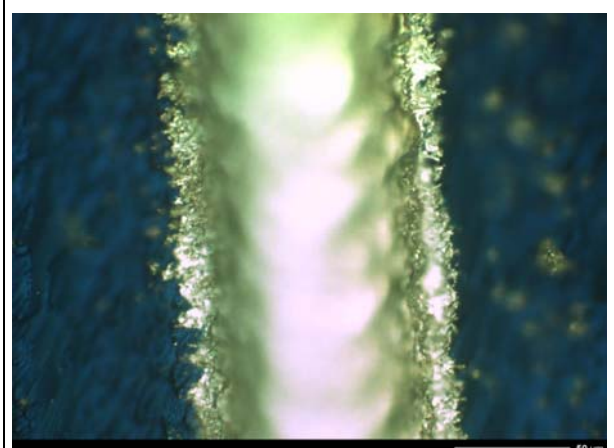
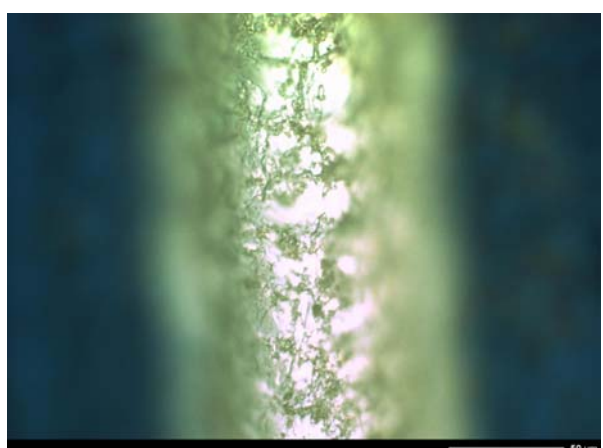
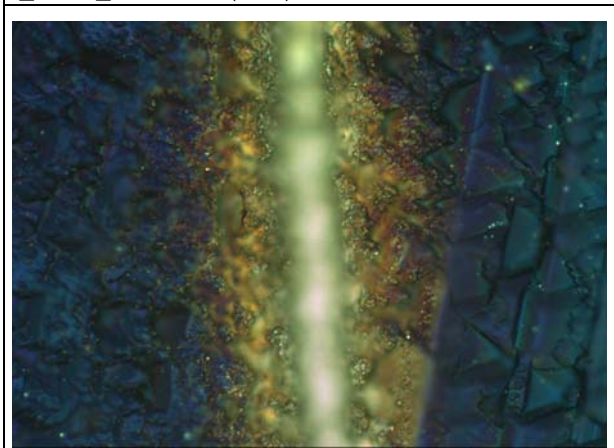
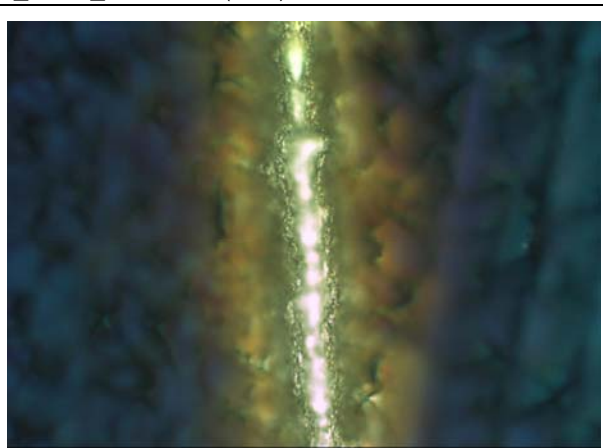


variant 11.:



2.5 Optical microscope images of edge isolation

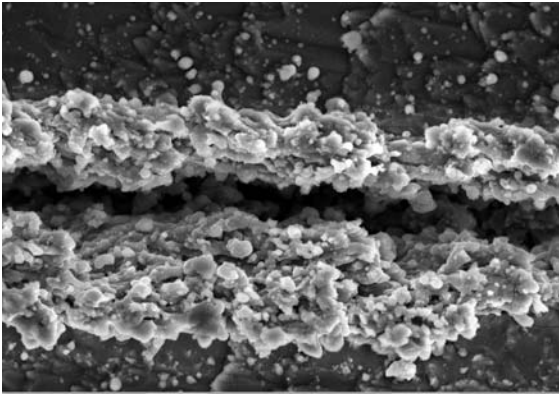
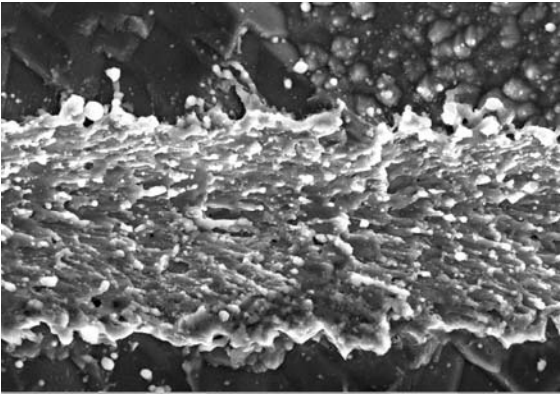
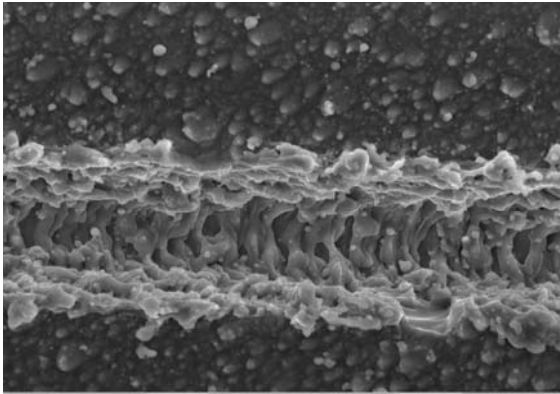
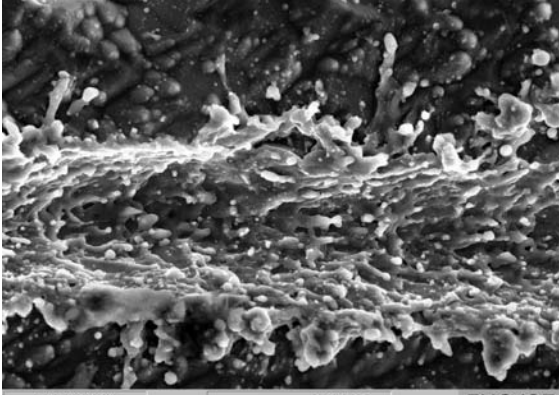
Table 4: Comparison of edge isolation variants

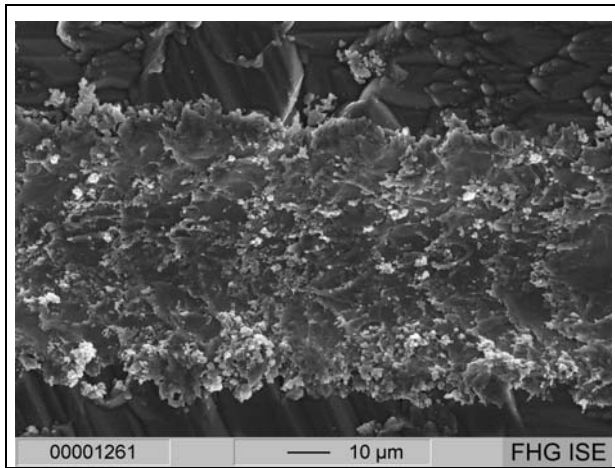
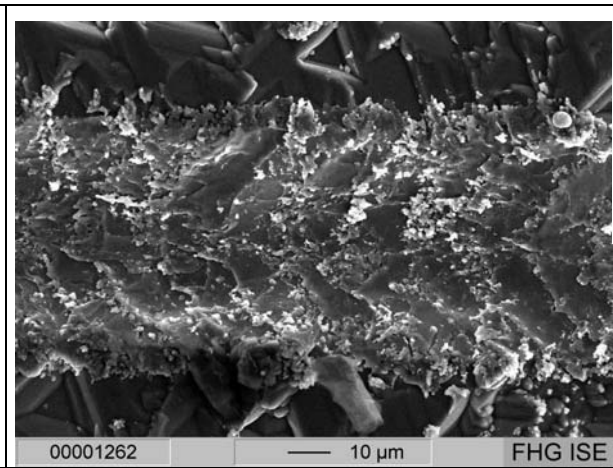
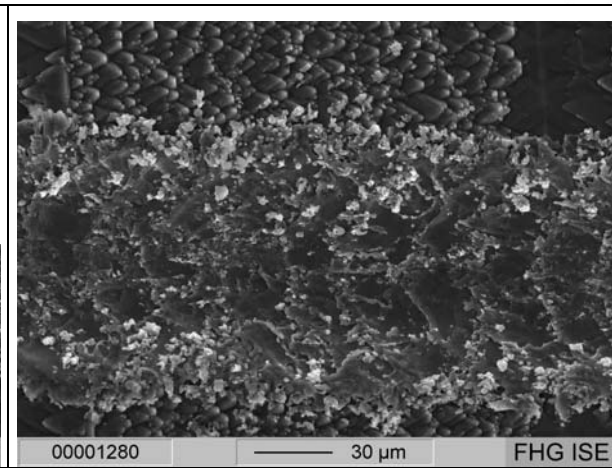
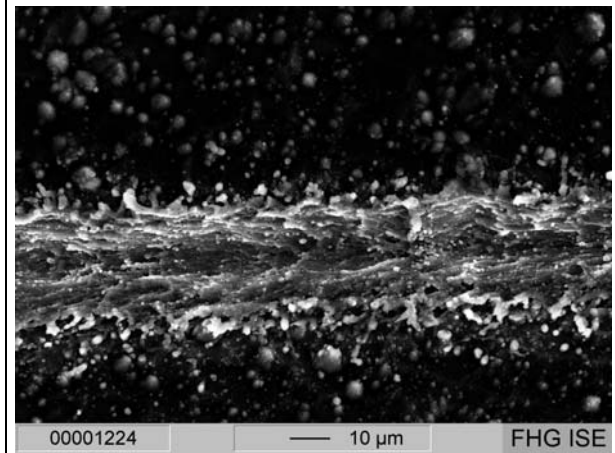
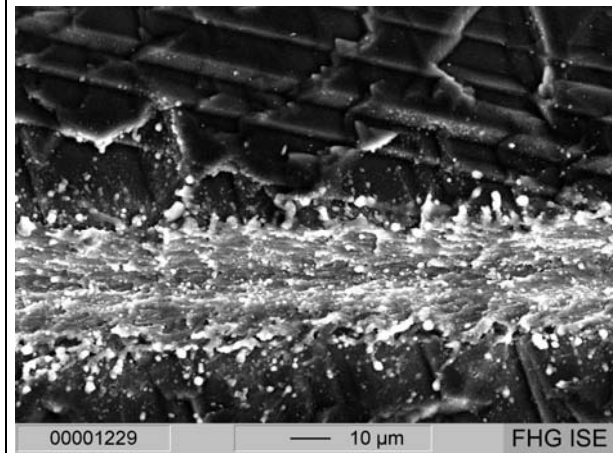
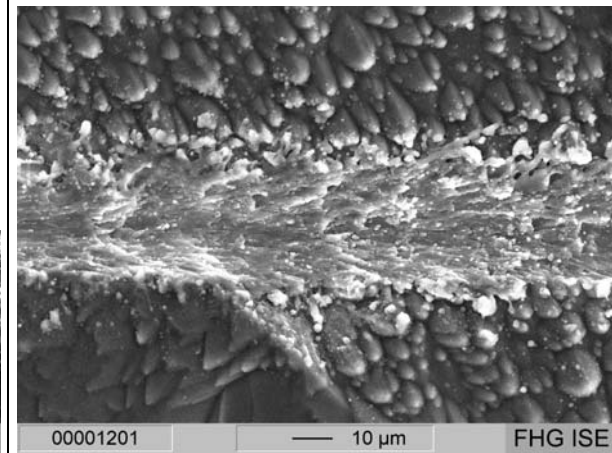
Groove of edge isolation; wafer surface	Groove of edge isolation; groove bottom
	
25 El_variant 1 (standard-industry)	25 El_variant 1 (standard-industry)
	
I_55 El_variant 6 (LMJ)	I_55 El_variant 6 (LMJ)
	
I_98 El_variant 12 (ISE UV)	I_98 El_variant 12 (ISE UV)

2.6 SEM images

Table 5 shows a comparison between the three different edge isolation processes. The laser groove of variant 1 is very inhomogeneous across the cell and a lot of molten silicon is ejected. Already less molten silicon can be noticed on the images of the ISE-EI with UV-laser and flying optics. Less ejected silicon is found with the LMJ process in comparison to the other process variants. Both ISE-EI and LMJ-EI are more homogeneous across the cell than the standard-industry process. In evidence: LMJ laser groove is much wider due to the 100 μm nozzle.

Table 5: SEM images of edge isolation variants

 <p>00001245 — 10 μm FHG ISE</p>	 <p>00001253 — 10 μm FHG ISE</p>	 <p>00001260 — 10 μm FHG ISE</p>
<p>16 EI_variant 1 (standard-industry)</p>	<p>16 EI_variant 1 (standard-industry)</p>	<p>16 EI_variant 1 (standard-industry)</p>
 <p>00001218 — 10 μm FHG ISE</p>		
<p>25 EI_variant 1 (standard-industry)</p>		

 <p>00001261 — 10 µm FHG ISE</p>	 <p>00001262 — 10 µm FHG ISE</p>	 <p>00001280 — 30 µm FHG ISE</p>
<p>I_55 EI_variant 6 (LMJ)</p>	<p>I_55 EI_variant 6 (LMJ)</p>	<p>I_55 EI_variant 6 (LMJ)</p>
 <p>00001224 — 10 µm FHG ISE</p>	 <p>00001229 — 10 µm FHG ISE</p>	 <p>00001201 — 10 µm FHG ISE</p>
<p>I_98 EI_variant 12 (UV ISE)</p>	<p>I_98 EI_variant 12 (UV ISE)</p>	<p>I_100 EI_variant 12 (UV ISE)</p>

2.7 Breakage test

To analyze the mechanical strength all cells were breakage tested with a Zwick BasicLine 4-line-bending apparatus. The maximum breakage force is detected.

The required breakage force is listed in table 6 and depicted in figure 1 for all EI-variants.

The broad distribution of the results is due to the small number of tested cells. It also indicates that only little large cracks were generated by the edge isolation (with numerous large micro cracks the breakage force would have constant smaller values). This is confirmed by the fact that the cell fragments are large. The cells don't split as it would be typical for high breakage strengths and high concentration of small micro cracks. This is visible especially for the standard-industry isolated cells. 30 cells were breakage tested and even so the standard deviation was approx. 50 %.

The assumption is that the breakage emanates from laser induced damage on the edge of the solar cell and thus the results depend primarily from the varying edge isolation induced damage by the single processes. Figure 2 shows the beginning of a break induced by laser processing.

The broad distribution of the ISE UV-laser process is smaller than the standard-industry EI. This is in line with the more homogeneous laser groove depicted by the SEM images.

It is also valid for variant 10 (LMJ EI process). With this variant the highest breakage forces and the smallest distributions are obtained. However the process is too slow for industrial application because the scanning speed was only 100 mm/sec. An interesting issue is that an increase in groove depths does not lead to a decrease in breakage force necessarily. Besides this good result for LMJ there also exist lots of variants with decreased breakage force.

Table 6: Required maximum breakage forces

EI-variant		F max N	Number of cells
1	Average value	8,8	30
	Standard deviation	4,4	
	Average value/ Standard deviation [%]	50,4	
2	Average value	5,0	7
	Standard deviation	3,6	
	Average value/ Standard deviation [%]	72,2	
3	Average value	6,4	7
	Standard deviation	4,5	
	Average value/ Standard deviation [%]	70,1	
4	Average value	8,1	7
	Standard deviation	4,2	
	Average value/ Standard deviation [%]	52,5	

5	Average value	7,5	7
	Standard deviation	4,6	
	Average value/ Standard deviation [%]	61,1	
6	Average value	6,6	7
	Standard deviation	4,2	
	Average value/ Standard deviation [%]	64,1	
7	Average value	7,0	7
	Standard deviation	4,3	
	Average value/ Standard deviation [%]	61,9	
8	Average value	7,2	7
	Standard deviation	5,2	
	Average value/ Standard deviation [%]	71,5	
9	Average value	9,2	7
	Standard deviation	5,1	
	Average value/ Standard deviation [%]	55,2	
10	Average value	11,6	7
	Standard deviation	3,8	
	Average value/ Standard deviation [%]	32,5	
11	Average value	8,9	7
	Standard deviation	4,8	
	Average value/ Standard deviation [%]	54,1	
12	Average value	8,39	10
	Standard deviation	3,31	
	Average value/ Standard deviation [%]	39,5	

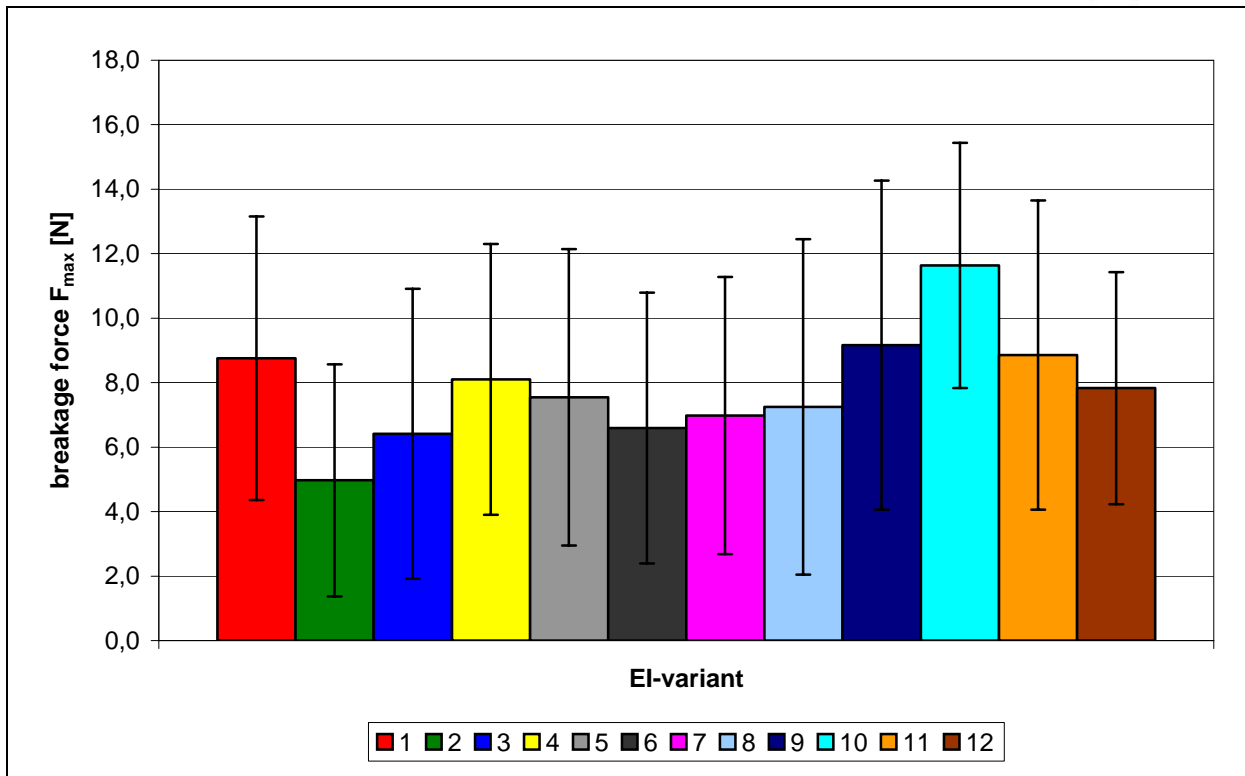


Figure 1: Comparison of the breakage forces of different EI-variants

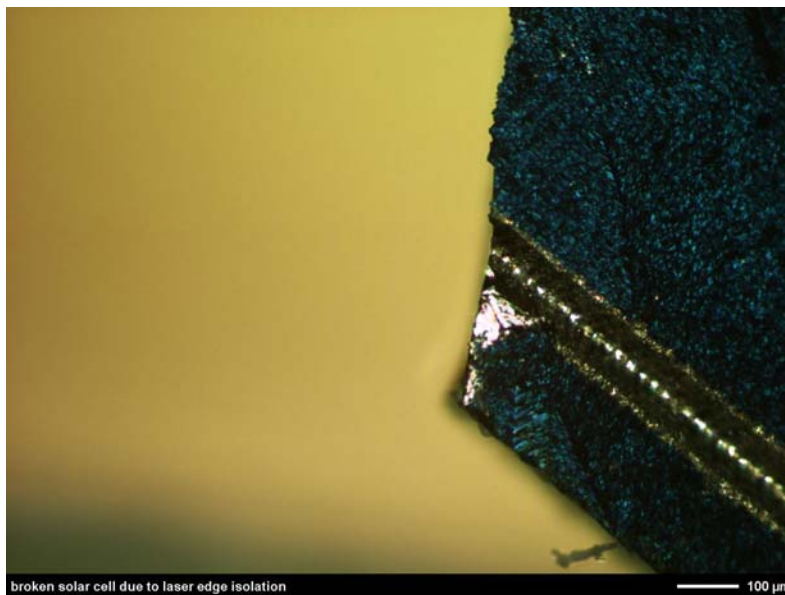


Figure 2: Onset of the breakage by a laser groove (EI-variant 2).

3 Conclusion

On the basis of the reached results one can say that the waterjet-guided laser Synova LaserMicroJet™ (LMJ) is suitable for the edge isolation of solar cells. The same electrical parameters than with the comparative standard laser processes can be achieved.

The highest fill factors of the tested solar cells are obtained with the LMJ, but the number of processed cells per variant is too low to get good statistical information. A further improvement of the standard laser is expected by optimization of the flying optic-UV-laser process.

However it has to be emphasized that the LMJ has reached standard-industry results in spite of suboptimal parameters. The recent results of the LMJ can even exceed the standard-industry-process by using a UV-light source, a smaller nozzle and a laser-axis coupled CNC controller. Herewith edge isolation with lower recombination losses by reduced melt layer thickness, smaller groove widths and isolated cell edges can be performed.

The potential of the LMJ process could not be fully utilized in this study because of the absent availability of a UV-light source.

Even with this experimental barrier of the LMJ indications for an advanced process are noticed:

- Constant lower n_2 -values for LMJ, possibly caused by reduced emitter damage
- Single processes with higher breakage forces
- Back side edge isolation partly successful (fill factors are not optimal, but compensated by increase of current)
- Better groove quality and homogeneity

An enhancement of the LMJ to an industrial process for solar cell processing is suggestive from our point of view. The further development should tend to other light sources (532 nm / UV) and a combination of good electrical quality and increase of breakage strengths. These processes have to be validated then for hundreds of solar cells favored from multiple manufacturers. At the same time the edge isolation on the back side should also be investigated furthermore. Afterwards a machine development with adequate partners should be approached especially for the photovoltaic industry. The Fraunhofer ISE can accompany this development and can provide an industrial validity of the prototype in the PV-TEC (photovoltaic technology evaluation center), a complete research-line for solar cells.

Freiburg, 11th of August 2006